

# An *in Situ* NMR Study of the Mechanism for the Catalytic Conversion of Fructose to 5-Hydroxymethylfurfural and then to Levulinic Acid Using $^{13}\text{C}$ Labeled D-Fructose

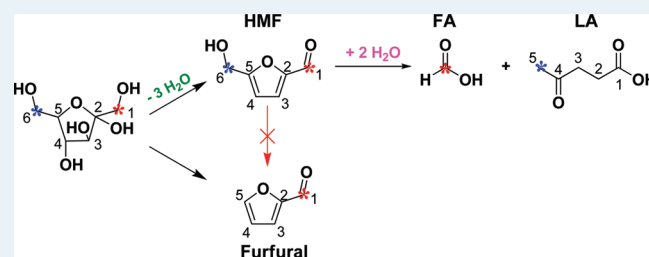
Jing Zhang and Eric Weitz\*

Department of Chemistry and Institute for Atom Efficient Chemical Transformation, Northwestern University, Evanston, Illinois 60208, United States

## Supporting Information

**ABSTRACT:** The pathways for the formation of 5-hydroxymethylfurfural (HMF) by dehydration of D-fructose and for the formation of levulinic acid and formic acid from HMF by rehydration were investigated by *in situ*  $^{13}\text{C}$  and  $^1\text{H}$  NMR using both unlabeled and  $^{13}\text{C}$ -labeled fructose. Water or DMSO was used as the solvent with Amberlyst 70,  $\text{PO}_4^{3-}$ /niobic acid, or sulfuric acid as catalysts. Only HMF is observed using NMR for fructose dehydration in DMSO with any of the three catalysts or without a catalyst. For each system, results with  $^{13}\text{C}$ -labeled fructose indicate that the first carbon (C-1) or sixth carbon (C-6) of fructose maps onto the corresponding carbons of HMF. For fructose dehydration in  $\text{H}_2\text{O}$  with a  $\text{PO}_4^{3-}$ /niobic acid catalyst, in addition to HMF, furfural was observed as a product. However, we show that furfural is not a reaction product deriving from HMF under our conditions. Rather our data indicate that there is a parallel reaction pathway open to fructose when the reaction takes place in  $\text{H}_2\text{O}$  with a  $\text{PO}_4^{3-}$ /niobic acid catalyst. The corresponding  $^{13}\text{C}$ -labeled results show that the first carbon in fructose maps onto the first carbon (aldehyde carbon) in furfural. Using  $^{13}\text{C}$ -enriched HMF formed from dehydration of  $^{13}\text{C}$ -labeled fructose in DMSO or  $\text{H}_2\text{O}$ , we investigated the pathway for HMF rehydration to levulinic and formic acid. The data in different solvents and with different catalysts are consistent with a common mechanism for HMF rehydration, which results in the C-1 and C-6 carbon of HMF being transformed to the carbon of formic acid and methyl carbon (C-5) of levulinic acid, respectively.

**KEYWORDS:** *in situ* NMR spectroscopy, isotope labeling studies, fructose dehydration, HMF rehydration



## INTRODUCTION

The consumption of fossil fuels has led to significant levels of environmental pollution, build up of atmospheric  $\text{CO}_2$ , and diminishing petrochemical reserves.<sup>1</sup> However, renewable biomass resources have the potential to provide a sustainable supply of fuels and chemical feedstocks.<sup>2–6</sup> Recently, substantial efforts have focused on converting biomass into 5-hydroxymethylfurfural (HMF),<sup>7–14</sup> due to HMF's potential versatility as an intermediate for the production of liquid alkanes, biofuels, furan-based chemicals,<sup>15–17</sup> and other potential chemical feedstocks, such as levulinic acid. A convenient method for the preparation of HMF is the acid-catalyzed dehydration of fructose, and this process is receiving increasing attention.<sup>18</sup> With an acid catalyst, HMF can then undergo rehydration to formic acid (FA) and levulinic acid (LA), which are versatile building blocks for the synthesis of various organic commodity chemicals and liquid transportation fuels.<sup>19</sup>

However, the dehydration of fructose to HMF and rehydration of HMF to LA and FA are complex multistep processes with many possible side reactions. Nevertheless, understanding the mechanisms for these processes is

fundamental to optimizing the yield of desired products and thus to improvements in biomass conversion. In general, the reaction pathways for the production of HMF from hexoses can involve isomerization, dehydration, fragmentation, reversion, and condensation steps.<sup>5</sup>

Two major reaction schemes for the production of HMF have been proposed. One is typically called the open-chain pathway<sup>20</sup> and involves two 1,2-eliminations and one 1,4-elimination of water. The second pathway involves a cyclic fructofuranosyl intermediate.<sup>21–23</sup> Based on  $^1\text{H}$  and  $^{13}\text{C}$  NMR data, Amarasekara et al.<sup>24</sup> identified a key cyclic intermediate as (4*R*,5*R*)-4-hydroxy-5-hydroxymethyl-4,5-dihydrofuran-2-carbaldehyde for fructose dehydration to HMF in  $\text{DMSO}-d_6$  at 150 °C, where the solvent act as the catalyst. Curtiss et al.<sup>25</sup> have recently reported on a high-level, CCSD-based (G4) quantum chemical investigation of the energies and reaction barriers for the dehydration of fructose through fructofuranosyl intermediates to produce HMF in neutral and acidic environments.

Received: January 20, 2012

Revised: March 22, 2012

Published: May 16, 2012

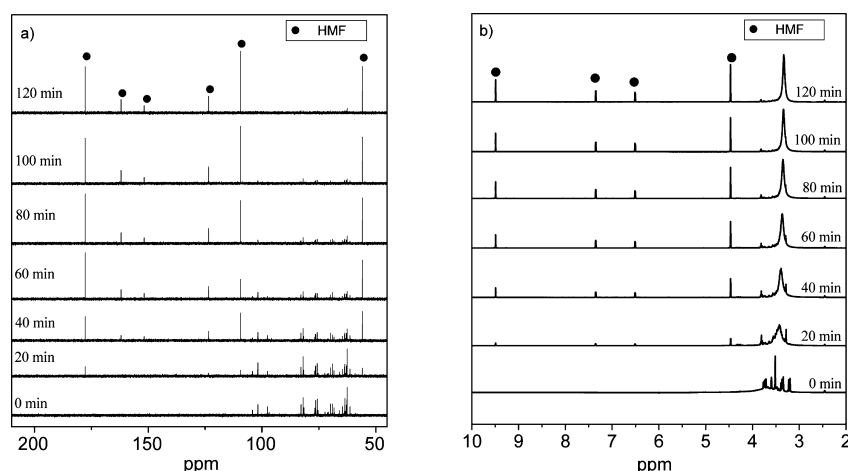


**Figure 1.** *In situ* (a)  $^{13}\text{C}$  NMR and (b)  $^1\text{H}$  NMR spectra as a function of time for the dehydration of 6 wt % fructose catalyzed by Amberlyst 70 in  $\text{DMSO-}d_6$  at  $95\text{ }^\circ\text{C}$ .

Though there have been several prior mechanistic investigations<sup>20–32</sup> of these industrially significant reactions, it is not clear that the mechanism for the conversion of fructose into HMF and then to LA and FA have been completely delineated at a molecular level, nor is it clear that the same mechanism is dominant with different catalysts in different solvents.

In this work, we employ *in situ* NMR to study the reactive behavior of fructose and HMF with Amberlyst 70,  $\text{PO}_4^{3-}$ /niobic acid, and sulfuric acid catalysts in two different solvents, DMSO and  $\text{H}_2\text{O}$ . We also employ fructose labeled with  $^{13}\text{C}$  at two positions and find that the first carbon or sixth carbon in fructose is initially converted to the first carbon (aldehyde carbon) or sixth carbon (methylene carbon) of HMF, and these labels are then converted to the carbon of FA and the fifth carbon (methyl carbon) of LA, respectively. We also report on the implications of our study for the mechanism of the reaction of fructose to form HMF.

## EXPERIMENTAL SECTION

**Materials and Instruments.** (–)-D-Fructose (>99.9%),  $\text{DMSO-}d_6$  (99.9% atom D),  $\text{D}_2\text{O}$  (99.9% atom D), phosphoric acid (85 wt %), 5-hydroxymethylfurfural (HMF) ( $\geq 99\%$ ), and sulfuric acid ( $\text{H}_2\text{SO}_4$ , 98 wt %) were obtained from Sigma–Aldrich and were used without further purification. Amberlyst 70 (sulfonic ion-exchange resin) was purchased from Sigma–Aldrich as wet beads and was dried in an oven at  $60\text{ }^\circ\text{C}$ . [ $^{13}\text{C-1}$ ]fructose and [ $^{13}\text{C-6}$ ]fructose (99 atom %) were purchased from Omicron Biochemicals Inc. (IN). Niobic acid ( $\text{Nb}_2\text{O}_5 \cdot n\text{H}_2\text{O}$ , containing 20 wt %  $\text{H}_2\text{O}$ ) was kindly supplied by CBMM (Companhia Brasileira de Metalurgia e Mineração). Preparation of the  $\text{PO}_4^{3-}$ /niobic acid catalyst followed procedures similar to those employed by Carlini et al.<sup>33</sup>

Liquid phase  $^{13}\text{C}$  and  $^1\text{H}$  nuclear magnetic resonance (NMR) spectra were obtained with a Varian Inova-400 spectrometer (400 MHz for  $^1\text{H}$ , 100 MHz for  $^{13}\text{C}$ ). When  $\text{DMSO-}d_6$  was used as solvent, chemical shifts (ppm) are reported relative to  $\text{DMSO-}d_6$ . When  $\text{H}_2\text{O}$  was used as solvent, 10 wt %  $\text{D}_2\text{O}$  was added by using the deuterium resonance of  $\text{D}_2\text{O}$  as the lock signal. Chemical shifts are relative to an external standard, 2,2-dimethyl-2-silapentane-3,3,4,4,5,5- $d_6$ -5-sulfonate sodium salt (DSS) for both  $^1\text{H}$  and  $^{13}\text{C}$  NMR.

**Procedures for *in Situ* NMR Studies. Fructose Dehydration in DMSO.** A solution of D-fructose (30 mg) and 20 mg

of the Amberlyst 70 beads in 0.5 mL of  $\text{DMSO-}d_6$  was prepared in a 5-mm J-Young NMR tube ( $\text{pH} \approx 6$ ). The solution was allowed to remain at room temperature for 12 h without mixing. The tube was then transferred to the NMR spectrometer, and  $^1\text{H}$  (rd = 2 s, NS = 16) and  $^{13}\text{C}$  (rd = 2 s, NS = 256) NMR spectra were recorded at room temperature. The NMR tube was then heated to  $95\text{ }^\circ\text{C}$ , and  $^{13}\text{C}$  and  $^1\text{H}$  NMR spectra were recorded using conditions identical to the  $t = 0$  spectrum, also taken at  $95\text{ }^\circ\text{C}$ . Afterward,  $^{13}\text{C}$  and  $^1\text{H}$  NMR spectra were recorded every 20 min for 2 h while keeping the temperature at  $95\text{ }^\circ\text{C}$ .

Similar procedures were followed for fructose dehydration in  $\text{DMSO-}d_6$  in the absence of an acid catalyst, as well as for  $\text{PO}_4^{3-}$ /niobic acid or sulfuric acid ( $\text{H}_2\text{SO}_4$ ) catalysts. For the  $\text{PO}_4^{3-}$ /niobic acid catalyst, the substrate/catalyst weight ratio was 1.5, and the mixture was sonicated after addition of the mixture to the NMR tube, while 10 mol % of  $\text{H}_2\text{SO}_4$  was used in  $\text{DMSO-}d_6$  at a reaction temperature of  $80\text{ }^\circ\text{C}$  ( $\text{pH} \approx 4$ ). The experimental procedure for  $^{13}\text{C}$ -labeled fructose was the same as described above for unlabeled fructose.

**Fructose Dehydration in  $\text{H}_2\text{O}$ .  $\text{PO}_4^{3-}$ /Niobic Acid Catalyst.** Similar procedures were followed for fructose dehydration in  $\text{DMSO-}d_6$  with the  $\text{PO}_4^{3-}$ /niobic acid catalyst, except that  $\text{H}_2\text{O}$  was used as the solvent (10 wt %  $\text{D}_2\text{O}$  was added).

**Amberlyst 70 or  $\text{H}_2\text{SO}_4$  Catalyst.** A solution of 50 mg of D-fructose (or [ $^{13}\text{C-1}$ ]fructose or [ $^{13}\text{C-6}$ ]fructose) and 50 mg of Amberlyst 70 in 0.45 mL of  $\text{H}_2\text{O}$ , to which 0.05 mL of  $\text{D}_2\text{O}$  was added, was prepared in a 5-mm J-Young NMR tube ( $\text{pH} \approx 6$ ). The tube was transferred to the NMR spectrometer, and  $^1\text{H}$  (rd = 2 s, NS = 16) and  $^{13}\text{C}$  (rd = 2 s, NS = 256) NMR spectra were recorded at room temperature. The tube was then heated and maintained at  $95\text{ }^\circ\text{C}$ , and  $^{13}\text{C}$  and  $^1\text{H}$  NMR spectra were recorded using conditions identical to the  $t = 0$  spectrum, which was also recorded at  $95\text{ }^\circ\text{C}$ . Then  $^{13}\text{C}$  and  $^1\text{H}$  NMR spectra were recorded every 2 h for the first 12 h and then periodically until 36 h. When  $\text{H}_2\text{SO}_4$  was used as the catalyst, similar procedures were followed, except that  $\text{H}_2\text{SO}_4$  was used as a 10 mol % solution ( $\text{pH} \approx 4$ ).

**HMF Rehydration to Levulinic Acid (LA) and Formic Acid (FA).** A solution of HMF (0.3 g), Amberlyst 70 (0.3 g), and solvent (10 mL of  $\text{DMSO-}d_6$  and  $\text{H}_2\text{O}$ , volume ratio 1:1) was charged into a 20 mL flask equipped with a magnetic stirrer

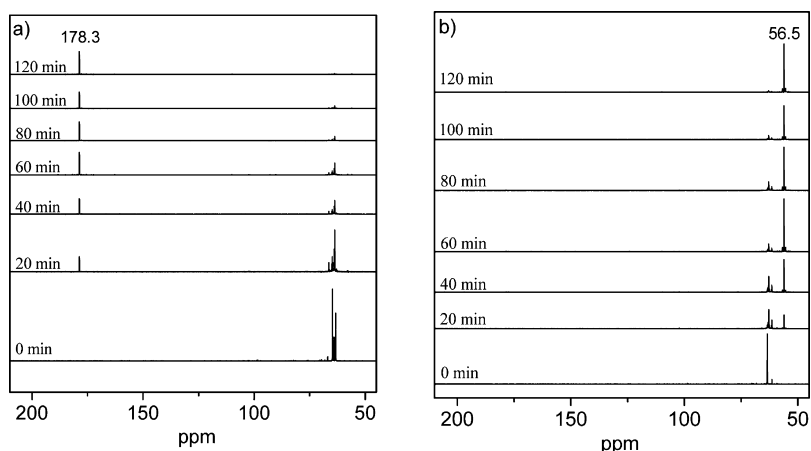


**Figure 2.** *In situ*  $^{13}\text{C}$  NMR spectra as a function of time for (a)  $^{13}\text{C}$ -1]fructose and (b)  $^{13}\text{C}$ -6]fructose dehydration catalyzed by Amberlyst 70 in  $\text{DMSO}-d_6$  at  $95\text{ }^\circ\text{C}$ .

and a condenser. The flask was heated to  $130\text{ }^\circ\text{C}$  with an oil bath while being stirred, and  $0.5\text{ mL}$  samples were periodically transferred to an NMR tube for up to  $30\text{ h}$  of reaction time. The reaction was quenched by immersing the NMR tube containing the sample in an ice–water bath, and  $^1\text{H}$  or  $^{13}\text{C}$  NMR spectra were sequentially recorded immediately thereafter.

Based on  $^{13}\text{C}$  and  $^1\text{H}$  NMR results, which are shown in Figure 1 and discussed in the next section, HMF is the only product observed from fructose dehydration in  $\text{DMSO}-d_6$  with Amberlyst 70 (or  $\text{H}_2\text{SO}_4$ ). Thus,  $^{13}\text{C}$ -labeled HMF was prepared *in situ* where  $^{13}\text{C}$ -1]fructose or  $^{13}\text{C}$ -6]fructose was dehydrated in  $\text{DMSO}-d_6$  with Amberlyst 70 at  $95\text{ }^\circ\text{C}$  (or  $\text{H}_2\text{SO}_4$  at  $80\text{ }^\circ\text{C}$ ). After the NMR tube was allowed to cool to room temperature,  $0.5\text{ mL}$  of  $\text{H}_2\text{O}$  was added to the J-Young NMR tube, and the NMR tube was put into the ultrasonic bath for  $5\text{ min}$  to mix the resulting solution. The J-Young NMR tube was then heated in a thermostatted oil bath at  $130\text{ }^\circ\text{C}$  for  $20\text{ h}$ . The reaction was then quenched by immersing the NMR tube in an ice–water bath, and the tube was immediately transferred to the NMR spectrometer, and  $^{13}\text{C}$  NMR spectra were recorded (Figures 6 and 7).

**HPLC Analysis of Reaction Mixtures.** Sample analysis was performed on a Agilent HPLC system equipped with a Wyatt Optilab T-rEX detector and a Bio-Rad Aminex HPX-87H ion exclusion column ( $300 \times 7.8\text{ mm}^2$ ).  $\text{H}_2\text{SO}_4$  ( $0.005\text{ M}$ ) was used as the mobile phase, which had a flow rate of  $0.55\text{ mL/min}$ . The column temperature was  $35\text{ }^\circ\text{C}$ , and the detector's temperature was set on  $35\text{ }^\circ\text{C}$ . The amount of fructose and HMF was determined using calibration curves.

## RESULTS AND DISCUSSION

**Characterization of the Pathway for HMF Formation from Fructose. Fructose Dehydration in DMSO.** Figure 1a shows a time progression of the *in situ*  $^{13}\text{C}$  NMR spectra for the dehydration of fructose to HMF with Amberlyst 70 in  $\text{DMSO}-d_6$  at  $95\text{ }^\circ\text{C}$ . The initial spectrum ( $t = 0\text{ min}$ ) exhibits NMR peaks between  $60$  and  $105\text{ ppm}$ , which have been assigned to the cyclic form of fructose ( $\beta$ -pyranose,  $\alpha$ -furanose, and  $\beta$ -furanose) in  $\text{DMSO}$ .<sup>34</sup> The  $^{13}\text{C}$  NMR spectrum recorded at  $t = 20\text{ min}$  ( $95\text{ }^\circ\text{C}$ ) is dominated by fructose NMR peaks, which are the only peaks seen in the initial spectrum, but peaks at  $56.5$ ,  $110.0$ ,  $124.6$ ,  $151.8$ ,  $162.0$ , and  $178.3\text{ ppm}$ , which are due to HMF, are now visible.<sup>35</sup> On increase of the reaction time

from  $40$  to  $100\text{ min}$ , the peaks due to HMF become larger, while the fructose peaks decrease in intensity. After  $2\text{ h}$ , the fructose peaks have virtually disappeared and the  $^{13}\text{C}$  NMR spectrum is dominated by HMF peaks.

The corresponding  $^1\text{H}$  spectra (Figure 1b) show similar results. The peaks between  $3.0$  and  $4.5\text{ ppm}$  are attributed to fructose (the peak at  $3.3\text{ ppm}$  is assigned to  $\text{H}_2\text{O}$  in  $\text{DMSO}-d_6$ ), while the peaks at  $4.47$  (s),  $6.50$  (d,  $J = 3.6\text{ Hz}$ ),  $7.40$  (d,  $J = 3.6\text{ Hz}$ ), and  $9.49$  (s) ppm are assigned to HMF.<sup>35</sup> As the reaction time is increased from  $20\text{ min}$  to  $2\text{ h}$  ( $95\text{ }^\circ\text{C}$ ), the peaks characteristic of HMF gradually increase while the peaks due to fructose decrease, as fructose dehydrates to produce HMF.

No signal due to other possible reactions products, such as levulinic acid or formic acid, was observed in either the  $^{13}\text{C}$  or  $^1\text{H}$  NMR spectra under these conditions. The  $^{13}\text{C}$  and  $^1\text{H}$  NMR spectra recorded after  $2\text{ h}$  showed only HMF signals, indicating that the fructose dehydration reaction in  $\text{DMSO}$  with Amberlyst 70 is selective for HMF formation relative to formic and levulinic acids. Experiments were also performed with fructose in  $\text{DMSO}-d_6$  with a sulfuric acid or a  $\text{PO}_4^{3-}$ /niobic acid catalyst or without an acid catalyst. In each case, based on both  $^{13}\text{C}$  and  $^1\text{H}$  NMR spectra, HMF is the only final product seen in the NMR spectra.

Musau et al.<sup>36</sup> suggested that  $\text{DMSO}$  associates with fructose and with water that is produced in the fructose dehydration reaction. Thus, subsequent reactions that involve the rehydration of HMF, such as the formation of LA and FA, may be greatly suppressed when  $\text{DMSO}$  is sufficiently in excess to associate with all the water released during the dehydration reaction. This is also likely a factor in a higher selectivity for HMF formation in  $\text{DMSO}$ <sup>1,11,12,37,38</sup> compared with  $\text{H}_2\text{O}$ , since with water as a solvent the reaction of fructose progresses beyond HMF to form LA and FA and insoluble humin formation is visible to the eye, though it is not detected by NMR.

In addition, HMF is relatively reactive under acidic conditions and elevated temperatures. However, the reactions in this work leading to formation of HMF were performed at  $95\text{ }^\circ\text{C}$  in the presence of a catalytic amount of acid. Thus, these mild conditions along with a low concentration of free water mitigate against substantial subsequent reactions of HMF. However, we do note that the color of the reaction solution changes from light yellow to dark yellow, and then to brown as the reaction time is increased from  $2$  to  $5\text{ h}$  (Supporting

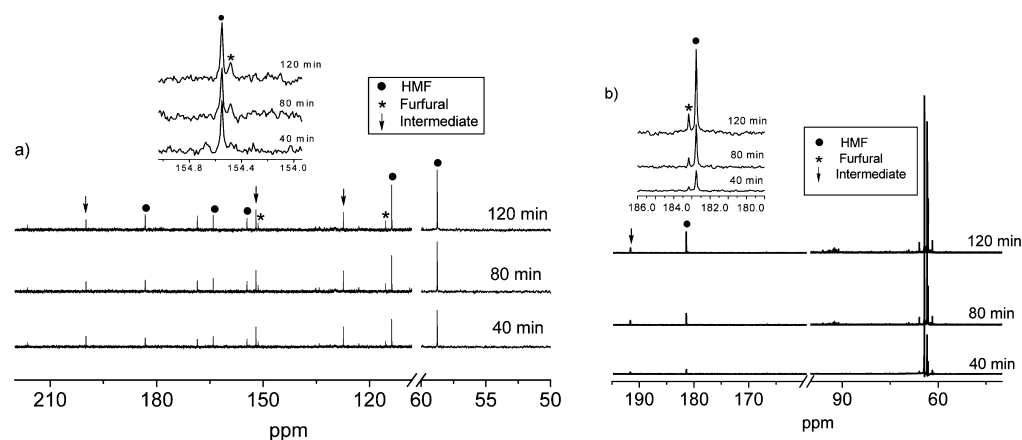


**Figure 3.** *In situ*  $^{13}\text{C}$  NMR spectra as a function of time for (a) fructose and (b)  $^{13}\text{C}$ -1 fructose dehydration in  $\text{H}_2\text{O}$  catalyzed by  $\text{PO}_4^{3-}$ /niobic acid at  $95^\circ\text{C}$ .

Information, Figure S1). Soluble polymers or insoluble humins are black, and as generally reported in the literature as such reactions proceed, the solution gradually becomes dark, presumably because of increasing amounts of polymers or humins.<sup>38</sup>

However, in our experiment no obvious insoluble humins are observed for reaction times of less than 5 h. Thus, the changes of the reaction solution color prior to this time may due to the polymerization of HMF or cross-polymerization between fructose and HMF, producing soluble polymers.<sup>38</sup> However, none of the polymeric species is apparent in the NMR spectra of the reaction system. The carbon balance, obtained from HPLC experiments, indicates that the sum of total carbon of identified products and nonreacted fructose accounts for at least 82% of total carbon in the initial fructose reactant using Amberlyst 70 as a catalyst and at least 65% when using a  $\text{PO}_4^{3-}$ /niobic acid catalyst. The carbon that is not detected by HPLC is likely incorporated in humins or polymeric materials that are formed during the reaction, which are either insoluble or adsorbed on the catalyst.

*In situ*  $^{13}\text{C}$  NMR was used to monitor where the first or sixth carbon (C-1 or C-6) in  $^{13}\text{C}$ -1 fructose or  $^{13}\text{C}$ -6 fructose resides in the HMF product. These results are displayed in Figure 2a,b, as a function of reaction time for the dehydration of  $^{13}\text{C}$ -1 fructose and  $^{13}\text{C}$ -6 fructose at  $95^\circ\text{C}$  in  $\text{DMSO}-d_6$  using an Amberlyst 70 catalyst. As seen in Figure 2a, the  $^{13}\text{C}$  NMR peaks (63.3, 64.0, and 64.6 ppm) of the C-1 carbons of the three main anomeric forms of D-fructose in  $\text{DMSO}$  are apparent in the baseline spectrum taken at  $t = 0$  min. For  $^{13}\text{C}$ -1 fructose dehydration at  $t = 20$  min, a peak in the carbonyl region at 178.3 ppm, assigned to the aldehyde carbon (C-1) in HMF, is greatly enhanced compared with other peaks characteristic of HMF, which are too weak to be visible in Figure 2a. Moreover, the peak at 178.3 ppm increases in intensity with increasing reaction time. These results indicate that C-1 carbon of fructose remains in the C-1 position in HMF.

The data in Figure 2b demonstrate that the NMR signals at 61.2, 63.0, and 63.2 ppm, due to the C-6 carbon in the three tautomers of fructose, are enhanced due to  $^{13}\text{C}$  enrichment. Spectra taken between 20 min and 2 h at  $95^\circ\text{C}$  indicate that the intensity of peak at 56.5 ppm, which belongs to the methylene carbon (C-6) in HMF, is enhanced relative to the intensities of other HMF NMR peaks, which are too weak to be

visible in Figure 2b. Thus, the C-6 carbon of fructose is the origin of the C-6 carbon of HMF.

The mapping of the  $^{13}\text{C}$  labels into HMF is compatible with what would be expected for this reaction based on the proposed generalized mechanism in refs 21–25. These results with regard to mapping of the  $^{13}\text{C}$  labels from fructose to HMF are the same as those obtained for the dehydration of  $^{13}\text{C}$ -1 fructose or  $^{13}\text{C}$ -6 fructose in  $\text{DMSO}$  with other catalysts ( $\text{H}_2\text{SO}_4$  or a  $\text{PO}_4^{3-}$ /niobic acid catalyst) or without a catalyst.

**Fructose Dehydration in  $\text{H}_2\text{O}$  with a  $\text{PO}_4^{3-}$ /Niobic Acid Catalyst.** As discussed, the dehydration of fructose to produce HMF takes place in  $\text{DMSO}$  with high yield and with a high degree of selectivity.<sup>36,39,40</sup> Of course, water would be a preferable solvent due to separation issues involved with the use of  $\text{DMSO}$ . But, with water there is a higher propensity to form LA and FA and byproducts. However, heterogeneous niobium-based catalysts not only show a high activity to produce HMF from fructose but have been shown to not efficiently rehydrate HMF to LA and FA in  $\text{H}_2\text{O}$ .<sup>33,41</sup> However, under these conditions, HMF formation is accompanied by the formation of a small amount of furfural.<sup>33</sup>

Figure 3a shows the *in situ*  $^{13}\text{C}$  NMR spectra for the dehydration of 6 wt % fructose in  $\text{H}_2\text{O}$  with  $\text{PO}_4^{3-}$ /niobic acid at  $95^\circ\text{C}$ . The  $^{13}\text{C}$  NMR (rd = 2 s, NS = 1024) spectra at  $t = 40$  min confirmed the production of HMF with the peaks at 58.2, 113.7, 154.5, 164.0, and 182.8 ppm, and the formation of furfural (115.4, 151.6, 154.4, 183.2 ppm) is also evident. In addition, two alkene peaks at 127.4 and 152.0 ppm and a peak in the carbonyl region at 195.0 ppm that are compatible with the proposed cyclic intermediate<sup>24</sup> are produced during the fructose dehydration reaction. In fact, this cyclic intermediate was found for all the systems (in  $\text{DMSO}$  or in  $\text{H}_2\text{O}$ ) we studied. This intermediate will be discussed in more detail in future work. As the reaction time is increased to 80 min, NMR peaks due to HMF and furfural become apparent.

Tao et al.<sup>42</sup> suggested that there are two pathways for the decomposition of HMF in the hydrolysis of cellulose catalyzed by an ionic liquid at  $150^\circ\text{C}$ . One pathway is the rehydration of HMF into LA and FA; the other is the loss of formaldehyde from HMF to yield furfural. However, Katō<sup>43</sup> suggested that HMF is not a major precursor for furfural production on pyrolysis of HMF at 350 and  $500^\circ\text{C}$ . A similar conclusion was reported by Tidwell et al.<sup>44</sup> on the hydrothermolysis of cellulose over the temperature range from 250 to  $350^\circ\text{C}$ . Thus, there is a debate in the literature as to whether HMF is a

precursor for furfural formation, though recent results seem to preponderantly support the conclusion that HMF is a precursor for furfural.<sup>42,45,46</sup>

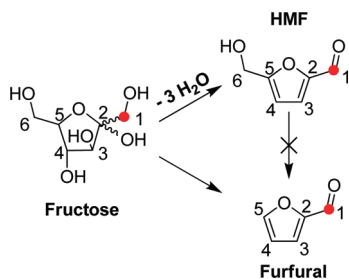
Our data show that furfural formation is not observed when HMF reacts in H<sub>2</sub>O with a PO<sub>4</sub><sup>3-</sup>/niobic acid catalyst. This result indicates that at least under our conditions, furfural is not a major reaction product deriving from HMF. Thus, we conclude that with a PO<sub>4</sub><sup>3-</sup>/niobic acid catalyst there is a parallel reaction pathway open to fructose when the fructose dehydration reaction takes place in H<sub>2</sub>O. One possible reaction mechanism has been reported by Krishna et al.,<sup>47</sup> who proposed a reaction mechanism that consists of isomerization of open chain D-fructose to 1,2-enediol, dehydration of the 1,2-enediol to 3-deoxy-hexosulose followed by dehydration and decomposition reactions forming formaldehyde, and another dehydration reaction to form furfural.

According to the mechanism proposed by Aida et al.,<sup>48</sup> furfural may be formed via tautomerization of open chain D-fructose to 2,3-enediol and then form a 3-ketose followed by a retro-aldol reaction forming formaldehyde and arabinose. Furfural can be formed from arabinose dehydration. We observe more open chain D-fructose with a niobic acid catalyst relative to the Amberlyst 70 catalyst (~3% versus ~1.5%). However, the furfural signal observed as a product of the reaction with a niobic acid catalyst at 95 °C is well beyond a factor of 2 above the detection limit. Thus, if the formation of furfural only depended on the amount of the open chain D-fructose isomer, we would expect to see furfural formation in both systems. Then, the fact that we do not observe furfural with Amberlyst 70 suggests that there is a difference in reaction pathways for the two catalysts. This result has interesting ramifications with regard to the effect of different catalysts on the barriers for potentially competing fructose reaction pathways.

When [<sup>13</sup>C-1]fructose (Figure 3b) or [<sup>13</sup>C-6]fructose (data not shown) is used under the same conditions as above, <sup>13</sup>C NMR indicates that the C-1 or C-6 carbon of fructose is the origin of the C-1 or C-6 carbon of HMF, respectively, which is in agreement with the results for fructose dehydration in DMSO. In addition, as seen in Figure 3b, the NMR signal at 183.2 ppm due to the aldehyde carbon (C-1) in furfural is enhanced, demonstrating that the first carbon in fructose maps onto the first carbon in furfural, as illustrated in Scheme 1.

**Fructose Dehydration in H<sub>2</sub>O with an Amberlyst 70 or H<sub>2</sub>SO<sub>4</sub> Catalyst.** <sup>13</sup>C and <sup>1</sup>H NMR were used for *in situ* (Figure 4) monitoring of the conversion of fructose in H<sub>2</sub>O with Amberlyst 70 at 95 °C. During the first 4 h, in addition to resonances due to fructose, only the resonance attributed to HMF is apparent. The <sup>13</sup>C NMR resonances in Figure 4a at

**Scheme 1. A Proposed Schematic Mechanism for Furfural Formation from Fructose Dehydration**



27.7, 29.0, 37.6, 178.0, and 215.0 ppm and the <sup>1</sup>H NMR peaks in Figure 4c at 2.04 (s), 2.39 (t, *J* = 5.1 Hz), and 2.67 ppm (t, *J* = 5.0 Hz)) are attributed to LA,<sup>49</sup> and the <sup>13</sup>C NMR resonance at 166.2 ppm (<sup>1</sup>H NMR peak at 8.05 ppm) is ascribed to FA.<sup>50</sup> Weak <sup>13</sup>C and <sup>1</sup>H NMR lines attributed to LA and FA become apparent after 6 h, and the amplitude of the HMF resonances peak at around 6 h of reaction time. An increase in the characteristic resonances associated with LA and FA are accompanied by a decrease in the intensity of the HMF peaks and a further decrease in the fructose resonances as the reaction further proceeds from 8 to 20 h.

After 36 h, the signals due to fructose and HMF have almost completely disappeared and only NMR peaks due to LA and FA are observed. However, we do not see evidence for furfural formation with Amberlyst 70 under these reaction conditions. It should be noted that although no insoluble humins are evident in the solution during the reaction of fructose in H<sub>2</sub>O, the Amberlyst 70 catalyst turns from brown to black during the reaction. A UV Raman spectrum (Supporting Information, Figure S2) of the used Amberlyst 70 catalyst shows a shift in the observed major peaks at 1390 and 1613 cm<sup>-1</sup> when compared with the fresh catalyst. This shift is likely indicative of the deposition of humins<sup>51,52</sup> on the surface of Amberlyst 70.

Under the same experimental conditions as above for Amberlyst 70 in H<sub>2</sub>O, HMF is the dominant product for the first 4 h when [<sup>13</sup>C-1]fructose or [<sup>13</sup>C-6]fructose is used as a starting material (Figure 5a,b respectively). The reaction of [<sup>13</sup>C-1]fructose or [<sup>13</sup>C-6]fructose leads to a strong <sup>13</sup>C resonance at 182.8 or 58.2 ppm in Figure 5a,b, which is attributed to the C-1 or C-6 carbon of HMF, respectively. This indicates that the C-1 or C-6 carbon of fructose ends up as the C-1 or C-6 carbon of HMF for fructose dehydration in H<sub>2</sub>O using Amberlyst 70 as a catalyst, as was seen for HMF formation from fructose dehydration in DMSO (Figure 2) and HMF formation in H<sub>2</sub>O with a PO<sub>4</sub><sup>3-</sup>/niobic acid catalyst (Figure 3).

After 6 h reaction time for [<sup>13</sup>C-1]fructose in H<sub>2</sub>O with the Amberlyst 70 catalyst, in addition to C-1 peaks of HMF and fructose (Figure 5a), a resonance at 166.2 ppm, which is attributed to FA, is observable. Longer reaction time (8–20 h) leads to an increase in intensity of the 166.2 ppm resonance and a decrease in intensity of the resonances associated with HMF and fructose. These results demonstrate that the first carbon (C-1) in HMF ends up as the carbon in formic acid. As seen in Figure 5b, after 6 h reaction time for [<sup>13</sup>C-6]fructose in H<sub>2</sub>O, two intense resonances, at 29.0 and 58.2 ppm, which are ascribed to LA and HMF, are observed in addition to C-6 peaks due to fructose. This indicates that the C-6 carbon in fructose is initially converted to the C-6 carbon of HMF, and it is then converted to the methyl carbon (C-5) of LA.

When H<sub>2</sub>SO<sub>4</sub> is used as a catalyst for fructose conversion in H<sub>2</sub>O (not shown), <sup>13</sup>C and <sup>1</sup>H NMR signals due to HMF increase for the first hour and begin to decrease on longer time scales as the NMR signals due to LA and FA increase. Only LA and FA are observed as final products in the NMR spectra. However, obvious insoluble humins are observed during the reaction for fructose conversion with the H<sub>2</sub>SO<sub>4</sub> catalyst. When <sup>13</sup>C-enriched fructose was used as a precursor for fructose conversion in H<sub>2</sub>O with either H<sub>2</sub>SO<sub>4</sub> or an Amberlyst 70 catalyst, the same behavior as discussed above with regard to the mapping of <sup>13</sup>C labels onto HMF and then to LA and FA is observed. With <sup>13</sup>C-enriched fructose ([<sup>13</sup>C-1]fructose or [<sup>13</sup>C-6]fructose) the C-1 and C-6 carbon of fructose is transformed

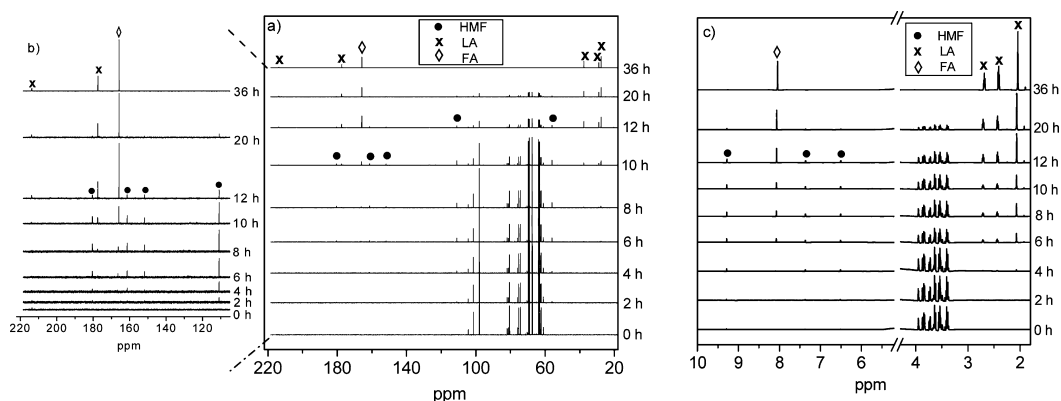


**Figure 4.** *In situ* NMR spectra as a function of time for the conversion of 10 wt % fructose catalyzed by Amberlyst 70 in H<sub>2</sub>O at 95 °C: (a) <sup>13</sup>C NMR spectra; (b) enlarged <sup>13</sup>C NMR spectra between 105 and 220 ppm; (c) <sup>1</sup>H NMR spectra. In panels a and b, the intensity of <sup>13</sup>C NMR spectrum taken at 36 h is divided by 3, while the intensity of <sup>1</sup>H NMR spectrum taken at 36 h in panel c is divided by 2.

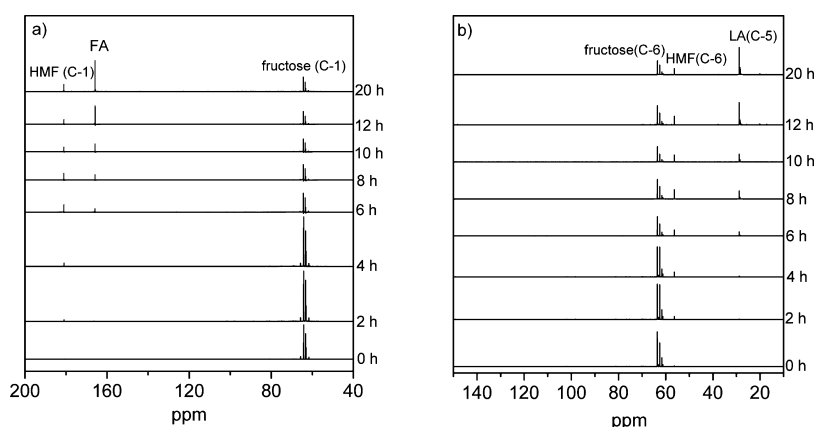


**Figure 5.** *In situ* <sup>13</sup>C NMR spectra as a function of time for (a) [<sup>13</sup>C-1]fructose and (b) [<sup>13</sup>C-6]fructose conversion in H<sub>2</sub>O catalyzed by Amberlyst 70 at 95 °C.

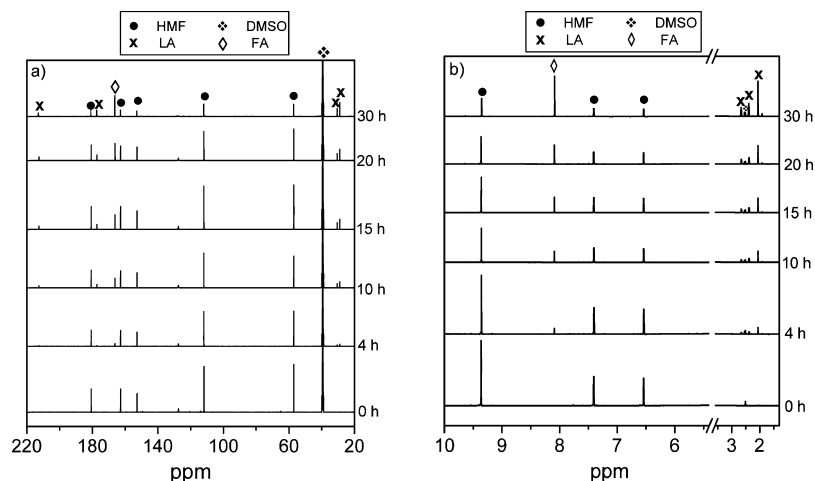


**Figure 6.** <sup>13</sup>C NMR spectra (a) and <sup>1</sup>H NMR spectra (b) as a function of time for 3 wt % HMF rehydration catalyzed by Amberlyst 70 in a mixture of DMSO-*d*<sub>6</sub> and H<sub>2</sub>O (volume ratio 1:1). The reaction took place at 130 °C, and the spectra were recorded at room temperature.

to the C-1 and C-6 carbon of HMF and then to the carbon of formic acid and the C-5 carbon of levulinic acid, respectively.

**Characterization of the Pathway of the HMF Rehydration to Levulinic Acid (LA) and Formic Acid (FA).** LA and FA can be obtained from the rehydration of HMF, but the reaction mechanism is still not well understood. Horvat et al.<sup>31</sup> proposed a mechanism based on <sup>13</sup>C NMR

measurements with two distinct reaction pathways. One reaction pathway is proposed to lead to the formation of 2,5-dioxo-3-hexenal, which undergoes decomposition to LA and FA. The other reaction route is proposed to result in the formation of 2,5-dioxo-6-hydroxy-hexanal, leading to humins formation. More recently, Patil et al.<sup>53</sup> suggested that aldol addition and condensation involving 2,5-dioxo-6-hydroxy-

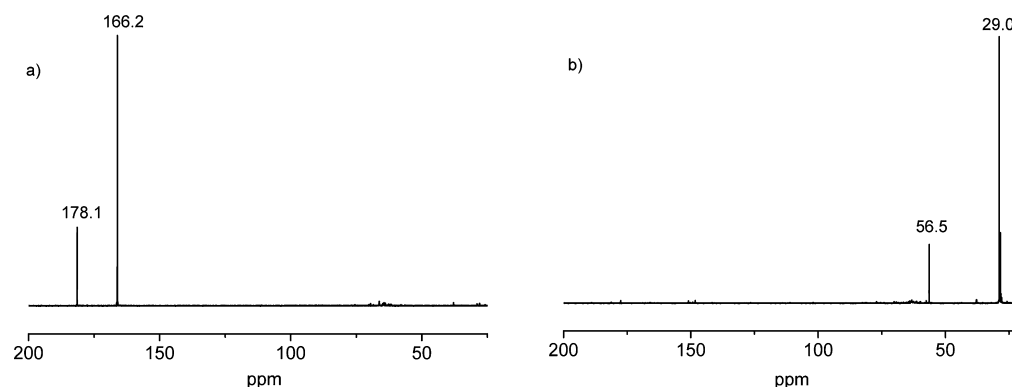


**Figure 7.**  $^{13}\text{C}$  NMR spectra of (a)  $[^{13}\text{C-1}]\text{HMF}$  and (b)  $[^{13}\text{C-6}]\text{HMF}$  rehydration in a mixture of  $\text{DMSO-}d_6$  and  $\text{H}_2\text{O}$  with an Amberlyst 70 catalyst (volume ratio 1:1). The reaction took place at  $130\text{ }^\circ\text{C}$ , and the spectra were recorded at room temperature.

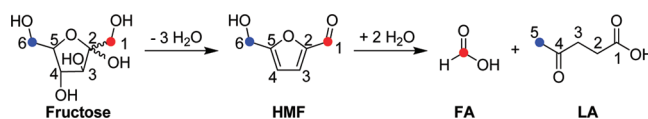
hexanal are important steps in the acid-catalyzed growth of humins.

In our experiments,  $[^{13}\text{C-1}]\text{HMF}$  or  $[^{13}\text{C-6}]\text{HMF}$  is formed when  $[^{13}\text{C-1}]\text{fructose}$  or  $[^{13}\text{C-6}]\text{fructose}$  is used as the precursor for fructose dehydration (Figure 2a,b) in DMSO, respectively. Figure 6a,b presents  $^{13}\text{C}$  and  $^1\text{H}$  NMR spectra, respectively, for the rehydration reaction using 3 wt % HMF and an Amberlyst 70 catalyst in a mixture of  $\text{DMSO-}d_6$  and  $\text{H}_2\text{O}$  at  $130\text{ }^\circ\text{C}$ . The addition of water is necessary to allow the reaction of fructose to progress beyond HMF, which is where the reaction would terminate in DMSO. The resonances due to LA and FA become apparent in the spectra in Figure 6a,b taken at 4 h. With increasing reaction time, the peaks due to LA and FA increase in amplitude while those due to HMF decrease in amplitude. It is interesting to note that LA and FA are the only two products observed from NMR for HMF rehydration with Amberlyst 70. However, humin formation does occur since humins can be detected on Amberlyst 70 using Raman spectroscopy (See Figure S2, Supporting Information).

Figure 7a,b displays the  $^{13}\text{C}$  NMR spectrum for the rehydration of  $[^{13}\text{C-1}]\text{HMF}$  and  $[^{13}\text{C-6}]\text{HMF}$ , respectively, in a mixture of  $\text{DMSO-}d_6$  and  $\text{H}_2\text{O}$  with Amberlyst 70 at  $130\text{ }^\circ\text{C}$  after 20 h reaction time. A 166.2 ppm peak due to FA is enhanced in addition to the C-1 peak due to HMF (178.1 ppm) when  $[^{13}\text{C-1}]\text{HMF}$  is used as the reactant, indicating that the C-1 carbon in HMF ends up in FA. This suggests that the transformation of HMF to formic acid involves breaking a C1–C2 bond in HMF. For  $[^{13}\text{C-6}]\text{HMF}$  (Figure 7b), two strong NMR lines, at 29.0 and 56.5 ppm, which are assigned to the C-5 carbon of LA and C-6 of HMF, were observed, indicating that the C-6 carbon in HMF maps onto the C-5 carbon in LA. These results are consistent with those discussed above utilizing  $^{13}\text{C}$ -enriched fructose (Figure 5a,b) in  $\text{H}_2\text{O}$  with an Amberlyst 70 catalyst.

The same results (not shown) with regard to the final positions of the  $^{13}\text{C}$ -labeled atoms were obtained when  $\text{H}_2\text{SO}_4$  was used as a catalyst for HMF rehydration in a mixture of  $\text{DMSO-}d_6$  and  $\text{H}_2\text{O}$ . However, the formation of insoluble humins was visually obvious with  $\text{H}_2\text{SO}_4$ . With the set of results that we have obtained for labeled fructose and HMF, a common schematic mechanism, shown in Scheme 2, is proposed for the catalytic conversion of fructose to HMF and then to LA and FA.

### Scheme 2. A Proposed Schematic Mechanism for the Catalytic Conversion of Fructose to HMF and then to Levulinic and Formic Acids



## CONCLUSIONS

The selective conversion of carbohydrates into useful chemical feedstocks, such as HMF and levulinic acid, is a complex but important chemical problem with a direct impact on energy and environmental problems. Our studies have focused on the pathways for the dehydration of fructose to HMF and its subsequent rehydration to form levulinic acid and formic acid in  $\text{H}_2\text{O}$  or in DMSO with different catalysts (Amberlyst 70,  $\text{PO}_4^{3-}/\text{niobic acid}$ , or sulfuric acid). We have utilized fructose enriched in  $^{13}\text{C}$  at various positions to obtain mechanistic insights. Fructose dehydration to HMF follows a similar mechanism in different solvents and with different catalysts, in which the C-1 or C-6 carbon of fructose maps onto the corresponding carbons of HMF. The results from these studies are consistent with a published proposed cyclic mechanism for the conversion of fructose into HMF<sup>21–25</sup>. However, furfural formation is observed in  $\text{H}_2\text{O}$  with a  $\text{PO}_4^{3-}/\text{niobic acid}$  catalyst. Moreover, under our reaction conditions furfural is not derived from HMF. This demonstrates that a parallel reaction pathway from fructose to furfural can be accessed with a niobic acid catalyst in water. This result further suggests that this latter catalytic system suppresses the energy barrier for the reaction pathway for furfural formation more efficiently than the other catalytic systems that we have used.

$^{13}\text{C}$ -labeled HMF produced via the reaction of  $^{13}\text{C}$ -labeled fructose was used to probe the pathway of the HMF rehydration in different solvents and for different catalysts. These results demonstrate that the C-1 and C-6 carbon of HMF is mapped onto the carbon of formic acid and C-5 carbon of levulinic acid, respectively. This mapping of the  $^{13}\text{C}$ -labeled HMF into LA and FA is also consistent with a published proposed generalized mechanism.<sup>21–25,31</sup>

## ASSOCIATED CONTENT

### Supporting Information

The color changes for the fructose dehydration reaction in  $\text{DMSO-}d_6$  at  $95\text{ }^\circ\text{C}$  using an Amberlyst 70 catalyst and a detailed description of UV Raman characterization techniques

and the UV Raman spectrum of the Amberlyst 70 catalyst along with a spectrum of the catalyst after it has been used for this reaction in water at 95 °C. This material is available free of charge via the Internet at <http://pubs.acs.org>.

## AUTHOR INFORMATION

### Corresponding Author

\*E-mail: [weitz@northwestern.edu](mailto:weitz@northwestern.edu).

### Notes

The authors declare no competing financial interest.

## ACKNOWLEDGMENTS

The authors thank Dr. Yuyang Wu of Northwestern University for NMR technical assistance. The authors also thank Dr. Taejin Kim from Chemical Sciences and Engineering Division, Argonne National Laboratory, for assistance with UV Raman measurements and analysis. This material is based upon work supported as part of the Institute for Atom-efficient Chemical Transformations (IACT), an Energy Frontier Research Center funded by the U.S. Department of Energy, Office of Science, Office of Basic Energy Sciences.

## REFERENCES

- (1) Roman-Leshkov, Y.; Chheda, J. N.; Dumesic, J. A. *Science* **2006**, *312*, 1933–1937.
- (2) Jae, J.; Tompsett, G. A.; Foster, A. J.; Hammond, K. D.; Auerbach, S. M.; Lobo, R. F.; Huber, G. W. *J. Catal.* **2011**, *279*, 257–268.
- (3) Ragauskas, J.; Williams, C. K.; Davison, B. H.; Britovsek, G.; Cairney, J.; Eckert, C. A.; Frederick, W. J., Jr.; Hallett, J. P.; Leak, D. J.; Liotta, C. L.; Mielenz, J. R.; Murphy, R.; Templer, R.; Tschaplinski, T. *Science* **2006**, *311*, 484–489.
- (4) Schmidt, L. D.; Dauenhauer, P. J. *Nature* **2007**, *447*, 914–915.
- (5) Tong, X. L.; Ma, Y.; Li, Y. D. *Appl. Catal., A* **2010**, *385*, 1–13.
- (6) Alonso, D. M.; Bond, J. Q.; Dumesic, J. A. *Green Chem.* **2010**, *12*, 1493–1513.
- (7) Ray, D.; Mittal, N.; Chung, W.-J. *Carbohydr. Res.* **2011**, *346*, 2145–2148.
- (8) Crisci, A. J.; Tucker, M. H.; Lee, M. Y.; Jang, S. G.; Dumesic, J. A.; Scott, S. L. *ACS Catal.* **2011**, *1*, 719–728.
- (9) Zhang, Y. M.; Degirmenci, V.; Li, C.; Hensen, E. J. M. *ChemSusChem* **2011**, *4*, 59–64.
- (10) Takagaki, A.; Takahashi, M.; Nishimura, S.; Ebitani, K. *ACS Catal.* **2011**, *1*, 1562–1565.
- (11) Qi, X. H.; Watanabe, M.; Aida, T. M.; Smith, R. L., Jr. *Ind. Eng. Chem. Res.* **2008**, *47*, 9234–9239.
- (12) Qi, X. H.; Watanabe, M.; Aida, T. M.; Smith, R. L., Jr. *Green Chem.* **2008**, *10*, 799–805.
- (13) Nikolla, E.; Roman-Leshkov, Y.; Moliner, M.; Davis, M. E. *ACS Catal.* **2011**, *1*, 408–410.
- (14) Hsu, W. H.; Lee, Y. Y.; Peng, W. H.; Wu, K. C.-W. *Catal. Today* **2011**, *174*, 65.
- (15) Casanova, O.; Iborra, S.; Corma, A. *J. Catal.* **2010**, *275*, 236–242.
- (16) Rosatella, A. A.; Simeonov, S. P.; Frade, R. F. M.; Afonso, C. A. M. *Green Chem.* **2011**, *13*, 754–793.
- (17) Roman-Leshkov, Y.; Dumesic, J. A. *Top. Catal.* **2009**, *52*, 297–303.
- (18) Carniti, P.; Gervasini, A.; Marzo, M. *Catal. Commun.* **2011**, *12*, 1122–1126.
- (19) Girisuta, B.; Janssen, L. P. B. M.; Heeres, H. J. *Trans IChemE, Part A, Chem. Eng. Res. Des.* **2006**, *84*, 339–349.
- (20) Moreau, C.; Durand, R.; Razigade, S.; Duhamet, J.; Faugeras, P.; Rivalier, P.; Ros, P.; Avignon, G. *Appl. Catal., A* **1996**, *145*, 211–224.
- (21) Antal, M. J., Jr.; Mok, W. S. L.; Richards, G. N. *Carbohydr. Res.* **1990**, *199*, 91–109.

- (22) Antal, M. J., Jr.; Leesomboon, T.; Mok, W. S.; Richards, G. N. *Carbohydr. Res.* **1991**, *217*, 71–85.
- (23) Li, C.; Zhao, Z. K.; Wang, A.; Zheng, M.; Zhang, T. *Carbohydr. Res.* **2010**, *345*, 1846–1850.
- (24) Amarasekara, A. S.; Williams, L. D.; Ebede, C. C. *Carbohydr. Res.* **2008**, *343*, 3021–3024.
- (25) Assary, R. S.; Redfern, P. C.; Greeley, J.; Curtiss, L. A. *J. Phys. Chem. B* **2011**, *115*, 4341–4349.
- (26) Haworth, W. N.; Jones, W. G. M. *J. Chem. Soc.* **1944**, 667–670.
- (27) Lewis, K. L. *J. Chem. Soc.* **1957**, 531–537.
- (28) Birkhofer, L.; Dutz, R. *Liebigs Ann. Chem.* **1957**, *608*, 7–17.
- (29) McKibbins, S. W.; Harris, J. F.; Saeman, J. F.; Neill, W. F. *Forest Prod. J.* **1962**, *19*, 17–23.
- (30) Kuster, B. F. M.; Tebbens, L. M. *Carbohydr. Res.* **1977**, *54*, 158–164.
- (31) Horvat, J.; Klaić, B.; Metelko, B.; Šunjic, V. *Tetrahedron Lett.* **1985**, *26*, 2111–2114.
- (32) Locas, C. P.; Yaylayan, V. A. *J. Agric. Food Chem.* **2008**, *56*, 6717–6723.
- (33) Carlini, C.; Giuttari, M.; Busca, G. *Appl. Catal. A: Gen.* **1999**, *183*, 295–302.
- (34) Nicole, D. J.; Gillet, B.; Eppiger, E. N.; Delpuech, J. J. *Tetrahedron Lett.* **1982**, *23*, 1669–1672.
- (35) Jiang, F.; Zhu, Q. J.; Ma, D.; Liu, X. M.; Han, X. W. *J. Mol. Catal. A: Chem.* **2011**, *334*, 8–12.
- (36) Musau, R. M.; Munavu, R. M. *Biomass* **1987**, *13*, 67–74.
- (37) Qi, X. H.; Watanabe, M.; Aida, T. M.; Smith, R. L. *Catal. Commun.* **2009**, *10*, 1771–1775.
- (38) Wang, F. F.; Shi, A. W.; Qin, X. X.; Liu, C. L.; Dong, W. S. *Carbohydr. Res.* **2011**, *346*, 982–985.
- (39) Nakamura, Y.; Morikawa, S. *Bull. Chem. Soc. Jpn.* **1980**, *53*, 3705–3706.
- (40) Seri, K.; Inoue, Y.; Ishida, H. *Chem. Lett.* **2000**, 22–23.
- (41) Nakajima, K.; Baba, Y.; Noma, R.; Kitano, M.; Kondo, J. N.; Hayashi, S.; Hara, M. *J. Am. Chem. Soc.* **2011**, *133*, 4224–4227.
- (42) Tao, F.; Song, H.; Chou, L. *Carbohydr. Res.* **2011**, *346*, 58–63.
- (43) Katō, K. *Agric. Biol. Chem.* **1967**, *31*, 657–663.
- (44) Kallury, R. K. M. R.; Ambidge, C.; Tidwell, T. T. *Carbohydr. Res.* **1986**, *158*, 253–261.
- (45) Shafizadeh, F.; Lai, Y. Z. *J. Org. Chem.* **1972**, *37*, 278–284.
- (46) Houminer, Y.; Patal, S. *Isr. J. Chem.* **1969**, *7*, 513–524.
- (47) Krishna, R.; Kallury, M. R.; Ambidge, C.; Tidwell, T. T.; Boocock, D. G. B.; Agblevor, F. A.; Stewart, D. J. *Carbohydr. Res.* **1986**, *158*, 253–261.
- (48) Aida, T. M.; Sato, Y.; Watanabe, M.; Tajima, K.; Nonaka, T.; Hattori, H.; Arai, K. *J. Supercrit. Fluids* **1997**, *40*, 381–388.
- (49) Yan, L. F.; Yang, N.; Pang, H.; Bin, L. *Clean* **2008**, *36*, 158–163.
- (50) Yoshida, K.; Wakai, C.; Matubayasi, N.; Nakahara, M. *J. Phys. Chem. A* **2004**, *37*, 7479–7482.
- (51) Bertarione, S.; Bonino, F.; Cesano, F.; Jain, S.; Zanetti, M.; Scarano, D.; Zecchina, A. *J. Phys. Chem. B* **2009**, *113*, 10571–10574.
- (52) Kim, T.; Assary, R. S.; Marshall, C. L.; Gosztola, D. J.; Curtiss, L. A.; Stair, P. C. *ChemCatChem* **2011**, *3*, 1451–1458.
- (53) Patil, S. K. R.; Lund, C. R. F. *Energy Fuels* **2011**, *25*, 4745–4755.

## NOTE ADDED IN PROOF

During final processing of this article a relevant article by G. R. Akien, L. Qi, and I. T. Horvath appeared as an accepted manuscript in *Chemical Communications* with a DOI 10.1039/C2CC31689G.